The Room Temperature Decomposition Mechanism of Dimethyl Methylphosphonate (DMMP) on Alumina-Supported Cerium Oxide − Participation of Nano-Sized Cerium Oxide Domains

Mark B. Mitchell,* Viktor N. Sheinker, Woodrow W. Cox, Jr., Enid N. Gatimu, and Aron B. Tesfamichael

Department of Chemistry and the Center for Surface Chemistry, Clark Atlanta University, Atlanta, Georgia 30314

Received: June 5, 2003; In Final Form: September 19, 2003

The adsorption and decomposition reactions of dimethyl methylphosphonate (DMMP) on cerium oxide supported on aluminum oxide have been examined at 25 °C. Experiments were carried out that involved dosing the reactive adsorbent with small doses of DMMP, followed by quantitative determination of the decomposition products. The results suggest that the formation reactions of methanol and dimethyl ether are competitive processes involving the same surface intermediate, which is most likely a surface methoxy species. Based on the observed results, it is proposed that the formation of dimethyl ether is due to the combination of two surface methoxy groups, while an important, if not the dominant, reaction producing methanol involves a surface methoxy group interacting with a vapor phase or physisorbed DMMP molecule. The presence of significant amounts of methoxy fragments formed upon DMMP adsorption is supported by results from diffuse reflectance spectroscopy, which also show that those groups are primarily associated with the cerium oxide domains. FT-Raman spectroscopy shows that the most active cerium oxide domains are highly dispersed two-dimensional domains or very small (<1 nm) crystallites. Somewhat larger (<6 nm) three-dimensional crystallites add to the decomposition yield, but less strongly. The FT-Raman evidence also supports the formation of a relatively narrow particle size distribution of cerium oxide crystallites on the alumina support surface from the sample preparation method. The alumina-supported cerium oxide reactive adsorbents developed as part of this study are the most active that have been reported in the literature for ambient temperature applications, decomposing approximately 775 μmol of DMMP per gram of adsorbent at 25 °C, and strongly or irreversibly adsorbing an additional 400 μmol, for a total capacity at room temperature of 1.1−1.2 mmol of DMMP per gram.

Introduction

Dimethyl methylphosphonate (DMMP) **I** is widely used as a simulant for pesticides and for chemical warfare agents, particularly for the study of the reactions on surfaces.[1,2] An understanding of the mechanism of decomposition of DMMP is critical for the development of materials such as powders, reactive fabrics, and coatings that can decompose chemical warfare agents at low temperatures, for the protection of personnel in the field who may have been exposed to such agents, for the detoxification of equipment and surfaces, and for the development of sensors for chemical warfare agents.[3] A number of groups have studied the interactions of DMMP with oxide surfaces at high temperatures for applications such as chemical warfare agent destruction and demilitarization of chemical weapons.[4−13] Others have examined the photochemical reactions of DMMP on photoactive surfaces for similar applications,[14−17] and several groups have examined the surface adsorption of DMMP for the development of chemical agent sensors.[18−22] Several studies have examined the decomposition of DMMP at ambient temperatures and lower.[23−31] Wagner and co-workers have investigated the interactions of VX, HD, and other chemical agents with nanosized Al_2O_3, MgO, and CaO.[32−34]

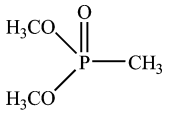

I

The mechanism typically used to describe the decomposition of DMMP on metal oxide surfaces is that proposed by Templeton and Weinberg in their examination of the interaction and reaction of DMMP and other phosphonates on alumina.[23,24] In those studies it was found that DMMP initially adsorbs at both Brønsted and Lewis acid sites through the phosphoryl oxygen. At room temperature, the interaction at Brønsted acid sites resulted in molecular adsorption. Dissociative adsorption at Lewis acid sites (coordinatively unsaturated aluminum sites) led to the formation of an adsorbed methyl methylphosphonate, with the second methoxy group presumably forming methanol either directly through reaction with a surface hydroxyl group, or via a two-step process with a surface methoxy group as an intermediate (Scheme 1). Once formed, the adsorbed methyl methylphosphonate fragment is not volatile and passivates the adsorption site(s) to which it is bound. Zhanpeisov et al. suggested in their computational study that gas-phase or adsorbed water could take the place of surface hydroxyl groups in the formation of methanol.[35] Dimethyl ether, also observed as a product, has been suggested to be the product of a

* Corresponding author. E-mail: mmitchel@cau.edu

10.1021/jp035590c CCC: $27.50
Published on Web 01/09/2004

SCHEME 1

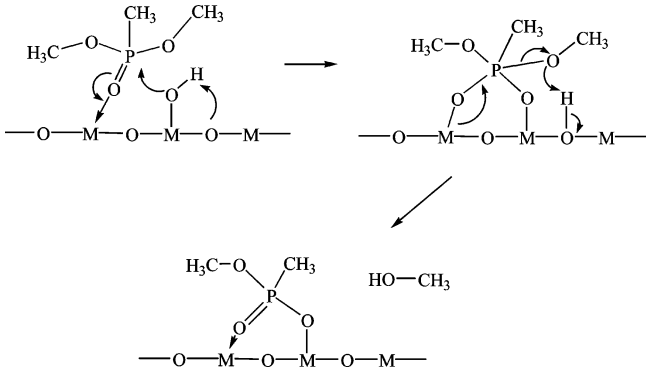

secondary, acid-catalyzed condensation reaction between two product methanol molecules.[26]

Previous investigations examining the room-temperature decomposition of DMMP in this laboratory[26,27] and in others, including Segal et al.[16] and Rusu and Yates,[29] have yielded results that are consistent with the mechanism suggested in Scheme 1. One mechanism requiring two DMMP molecules to yield gas-phase products has been proposed by Li and Klabunde[10] and Li et al.,[8] who suggested that, following decomposition of DMMP on magnesia to give an adsorbed methoxy group and an adsorbed methyl methylphosphonate, a second DMMP molecule could oxidize the adsorbed methanol, ultimately yielding formic acid as a reaction product.

The current study was undertaken to shed further light on the mechanism of decomposition of DMMP on these materials at room temperature, so that an accurate assessment of the amount of DMMP either decomposed or irreversibly adsorbed on the adsorbents could be developed from measurements of gas-phase products. In this study, the decomposition products from small aliquots of DMMP dosed onto a reactive adsorbent are measured as a function of the amount of added DMMP. The results observed are significantly different from those expected, and suggest that an isolated DMMP molecule on a metal oxide surface is unlikely to form gas-phase products. The observations are consistent with the formation of the observed dimethyl ether by the reaction between two surface methoxy fragments, and the formation of methanol from an interaction between a surface methoxy fragment and a mobile physisorbed or vapor-phase DMMP molecule. Additionally, the formation of significant amounts of surface methoxy fragments is indicated by the results from in situ infrared diffuse reflectance spectroscopy. FT-Raman spectroscopic results show that the form of the supported cerium oxide most active for decomposition is in the form of two-dimensional patches or very small (<1 nm) three-dimensional crystallites with additional decomposition activity provided by somewhat larger (<6 nm) crystallites that are formed as the cerium loading increases.

Experimental Section

The helium used for the study was a 99.9995% ultrahigh purity grade from Holox. DMMP was purchased from Aldrich and distilled under vacuum before use. The adsorbents were prepared using incipient wetness, or other aqueous-phase impregnation methods, with iron and cerium nitrates as the precursors and deionized water as the solvent. The alumina used was provided by UOP. Two different types were used, a γ-Al_2O_3 material called Versal GH (253 m^2/g) and a Bayerite material called Versal B that is transformed into an η-alumina on calcining (360 m^2/g). The η-alumina was chosen to provide an aluminum oxide support with a maximum surface area. While the two alumina materials show product formation from DMMP decomposition in approximately the same ratio as their surfaces (26.2 μmol of vapor-phase carbon formed for η-Al_2O_3 vs 19.1 μmol for the γ-Al_2O_3), there are some differences in the product branching ratio. When the DMMP decomposition is examined on pure η-Al_2O_3 with a continuous flow of DMMP, less than 3% of the total vapor-phase carbon produced is dimethyl ether, with the rest of the decomposition yield accounted for by the formation of methanol. Under the same conditions, the γ-Al_2O_3 DMMP decomposition yield is approximately 10% dimethyl ether and 90% methanol. These differences are probably accounted for by differences in surface acidity.

The impregnated γ-alumina samples were the same ones as described in an earlier publication and were prepared and analyzed as discussed in that reference.[27] The impregnated η-alumina samples were prepared using a method known as precipitation deposition, which has been used with success for the preparation of supported cerium oxide materials with high dispersion.[36,37] In this method, a dilute ammonia solution is slowly added to an aqueous solution of cerium nitrate, containing an appropriate amount of the substrate material, until all of the cerium has precipitated from solution (pH 9.5−10.0). Once filtered and dried, the supported oxide is formed upon calcining the solid in air at 400 °C. The cerium content was calculated from the amount of cerium and η-Al_2O_3 used in the impregnation solution, assuming complete conversion of the aqueous cerium precursor to supported oxide.

Microreactor Studies. The microreactor system has been described in detail previously, and only a short description is given here.[26] The microreactor consists of a 1/4 in. o.d. stainless steel u-tube in a controlled-temperature furnace, which is connected to a gas inlet system that carries the DMMP/He mixture to the reactor, and an exit system that carries the products to a 2.4 m long-path infrared gas cell for analysis. The inlet helium gas flow is controlled by a Teledyne-Hastings mass flow controller. The helium gas bubbles through liquid DMMP at a flow rate of 30 mL/min. After modification of the flow system, compared to that described in the earlier work, and recalibration of the DMMP flow, the DMMP concentration in the He stream has been determined to be 47.0 μmol/L. At a flow rate of 30.0 mL/min, the flow rate of DMMP was determined to be 1.41 μmol/min.

In the microreactor experiments, the adsorbent was placed near the bottom of the u-tube but on the entrance side. The adsorbent bed was composed of particles with a diameter of 90−250 μm, classified using standard testing sieves, and was supported on a porous stainless steel disk with 2 μm diameter pores (Mott Corporation). Prior to exposure to DMMP vapor, the adsorbent was heated to 400 °C in 20% O_2 in helium for 1 h, then in pure helium for 30 min. The adsorbent was then cooled to 25 °C in a pure helium flow. The DMMP vapor-generation system was contained in a temperature-controlled enclosure maintained at 25 °C. After the microreactor, the gas streamflowed to a long-path gas cell (Ultra-Mini Long Path Cell from Infrared Analysis, Inc.) with an effective path length of 2.4 m and an internal volume of 100 mL. Infrared spectra (Thermo-Nicolet Avatar 360 FT-IR), at 2 cm^{-1} resolution, were collected approximately every two minutes. The data analysis and product quantitation were carried out as in the earlier study. New to this study is the completion of the mass balance for the system. The DMMP breakthrough was calibrated by allowing small doses of DMMP to flow, at a known flow rate and concentration, into the infrared cell, and the infrared absorption

due to DMMP measured for a very long period of time, typically 24−28 h, so that all of the DMMP flows through the infrared cell. The integrated infrared signal then corresponds to the dose amount. A straight line fit for a series of integrated intensities vs dose amounts then formed the response curve for DMMP. The precision of the measurement is not as good as it is for the measurement of methanol and DMMP, but it is good enough to be able to draw important conclusions regarding the decomposition yields.

Experiments using the pure alumina materials were carried out multiple (more than three) times to evaluate the experimental setup and data analysis for reproducibility. Typically, an uncertainty of approximately ± 2 μmol is found for the determination of the integrated amount of methanol formed. The uncertainty found for dimethyl ether is less than that due to the fact that there are no interfering absorptions for the dimethyl ether gas-phase infrared absorption bands used for quantitation, while those of methanol are overlapped somewhat by DMMP absorptions.

Several different types of dosing experiments were carried out, and for each the pretreatment was carried out as described above. In the variable dose/fixed adsorbent experiment, 60 mg of the adsorbent was exposed to different dose amounts of DMMP. The dose amounts are formed by exposing the adsorbent to a flow of DMMP in He for an amount of time necessary to dose the sample with the predetermined amount of DMMP. The flow through the DMMP liquid is then stopped, and pure helium is directed to flow through the microreactor for the remaining time, at a constant flow rate of 30.0 mL/min. Typically, the flow of helium is continued for approximately 20 h (a total flow of helium of 36−37 L), compared to a dosing time of about 7 min for a 10 μmol dose of DMMP.

In the fixed dose/variable adsorbent experiment, several different amounts of adsorbent were exposed to fixed doses of DMMP, typically 20 μmol. The dose was again followed by a 20-hour continuous flow of pure helium and monitoring of products. The incremental dose/single adsorbent experiment was performed by dosing 60 mg of the adsorbent with successive 10 μmol doses of DMMP. Approximately 20 h were allowed to elapse between each dose, and infrared spectra were recorded continuously.

In Situ FT-IR Studies. The infrared diffuse reflectance studies were carried out in much the same way as described in an earlier publication.[38] The adsorbent to be examined was sieved and placed in a Harrick Scientific HVC-DR infrared diffuse reflectance controlled environment cell, the cell was closed and evacuated using an Alcatel diffusion pump. The sample was then exposed to a mixture of 20% O_2 in helium at 400 °C for approximately 30 min, and subsequently cooled to room temperature. All of the infrared spectra were collected using a Harrick Scientific DRA-2 optical accessory. After collection of a background spectrum, the dilute mixture of DMMP in helium (1:1000) was allowed to flow through the cell over the sample. The pressure in the cell during this time was approximately 500 mTorr. Spectra were measured during the adsorption process to monitor for DMMP adsorption using a Nicolet Magna 750 FT-IR and a liquid nitrogen cooled mercury−cadmium−telluride (MCT) detector. During adsorption, 250 scans at 8 cm^{-1} resolution (to minimize collection time) were co-added to form the spectra shown.

FT-Raman Studies. FT-Raman spectra were obtained using a Nicolet Raman 950 FT-Raman spectrometer using a laser power of approximately 250 mW. Raman scattered radiation was collected using a 180° backscattering collection geometry and detected using a room-temperature InGaAs detector. The neat powder samples were placed in capillary tubes for data collection.

Results

Microreactor Studies. Prior to describing the dosing experiments, it is useful to describe the results from several different control experiments that were carried out to help evaluate the results. In the first, a mixture of methanol in helium, 253 ppm from Matheson Gas, was allowed to flow continuously through the adsorbent bed at 25 °C. No conversion to dimethyl ether was observed, although conversion to dimethyl ether can be observed at 150 °C. Similarly, a mixture of dimethyl ether in helium, 490 ppm from Matheson Gas, gave no conversion to methanol at 25 °C. Finally, the DMMP in helium mixture flowing into an empty reactor did not yield any measurable decomposition products.

Initially, it was thought that 20−24 h would be more than sufficient to allow for all of the reaction products to flow from the adsorbent bed. In studies that we had carried out previously using the microreactor setup, both methanol and dimethyl ether were observed to flow from the bed relatively quickly.[26,27] However, those experiments were carried out using a continuous flow of DMMP, and the current experiments using small doses yield significantly different results as described below.

Variable Dose/Fixed Adsorbent Amount. A series of experiments was carried out on reactive adsorbents that had been examined in an earlier study.[27] These adsorbents were prepared using incipient wetness impregnation and included 7.5 wt % Ce and 5.0 wt % Fe co-impregnated on γ-Al_2O_3, 5.0 wt % Fe on γ-Al_2O_3, 7.5 wt % Ce on γ-Al_2O_3, and γ-Al_2O_3. The results for all of these adsorbents were similar and showed an apparent maximum in product formation of 23−27 μmol of product after exposure to an 80 μmol or larger dose of DMMP. The products formed represented a combination of dimethyl ether and methanol. For dose amounts less than 30 μmol of DMMP, the only product measured was dimethyl ether. Exposure to a 40−50 μmol dose of DMMP resulted, for most of the solids, in the observation of large amounts of methanol and diminishing amounts of dimethyl ether. These results led us to suspect that the processes leading to gas-phase products might be more complex than originally assumed.

A new series of reactive adsorbents was developed that showed significantly higher decomposition yields per gram of adsorbent. Our previous work showed that higher dispersions of CeO_2 yielded higher decomposition yields, and the precipitation deposition method used to prepare the new adsorbents in the current study had been shown by Soria and co-workers to yield high dispersions of supported cerium oxide.[36,37] The most reactive adsorbent had a composition of approximately 20 wt % Ce on η-Al_2O_3 and was used to obtain all of the microreactor results discussed. Samples with lower amounts of cerium showed lower decomposition yields as discussed in a later section. The decomposition product yield of DMMP as a function of DMMP dose for this adsorbent is shown in Figure 1A and B. These graphs show the amounts of methanol and dimethyl ether produced as a function of dose amount. The observation of products begins at somewhat lower doses on this solid than on those studied earlier, and the new solid is capable of forming approximately 44% more products than the previous formulations. These results are tabulated in Table 1.

The only product observed for the lowest doses of DMMP onto the solid, 10 and 20 μmol, is dimethyl ether. Figures 2 and 3 show the formation of the products of the DMMP

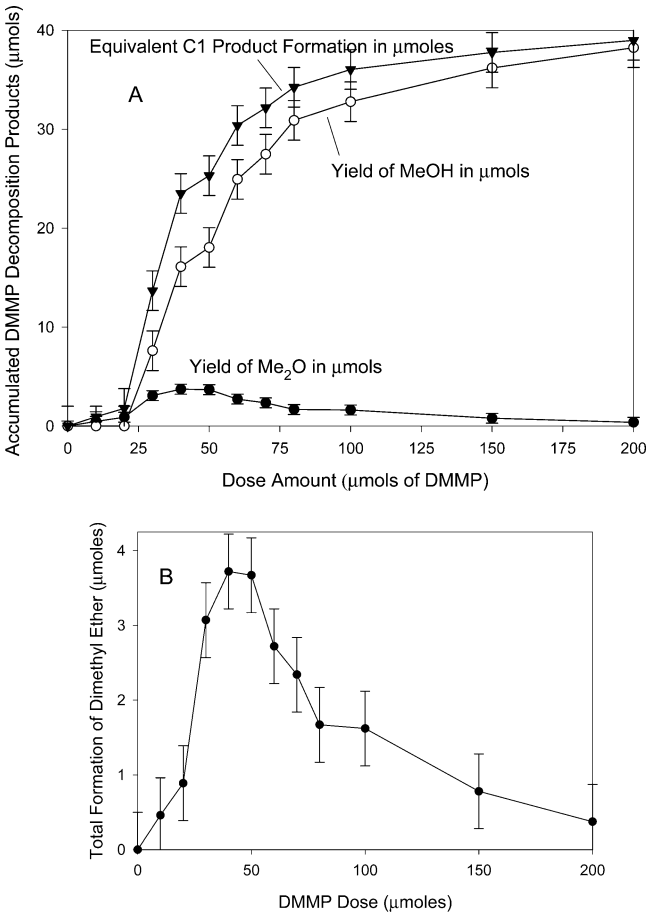

Figure 1. Decomposition products formed as a function of amount of DMMP dose for 20 wt % Ce on η-Al_2O_3. The error bars represent the estimated uncertainty associated with the determination of the amounts of reaction products formed. The error bars associated with the dimethyl ether are smaller since the infrared bands used to determine the dimethyl ether yield are free of interferences, especially those due to DMMP, whereas there is some overlap of the methanol infrared bands with those of DMMP.

decomposition reaction as a function of time for different DMMP doses. Included in Figure 2 is the measured DMMP flow for a 10 μmol dose of DMMP into an empty reactor (the long tail is due to the time needed to flush the DMMP from the gas cell). This provides an estimate of the DMMP concentration profile that the sample is exposed to. The results suggest that dimethyl ether formation is a relatively low probability event, because for a 20 μmol dose of DMMP, less than 1 μmol of dimethyl ether is produced. Also, it takes a long period of time for the dimethyl ether to evolve from the adsorbent bed, much longer than would have been predicted from our earlier studies.

The integrated product flow curves for DMMP doses of 30 to 200 μmol are shown in Figure 3A. These curves show the integrated product flow from the adsorbent as a function of time, where integrated product is expressed as the equivalent number of μmol of C_1 product formed, equal to the number of μmol of methanol plus two times the number of μmol of dimethyl ether. The initial product observed is dimethyl ether in all cases, and the time between the end of the dimethyl ether flow and the beginning of the methanol flow leads to the odd shape of the integrated product flow curves for the 30−50 μmol doses in Figure 3A. Figure 3B shows the integrated flow of methanol as a function of time.

DMMP breakthrough is observed only for dose amounts of 60 μmol and greater. The DMMP breakthrough curves (DMMP flow in μmol/min) are characterized by a broad asymmetric curve with a long tail. A significant change in the characteristics of the breakthrough curve occurs for dose amounts between 100 and 150 μmol; a strong, relatively narrow peak due to DMMP flow is superimposed on the leading edge of the broad DMMP flow curve observed for the lower doses. These results suggest that the surface can be very roughly characterized as being composed of two kinds of DMMP adsorption site, consistent with the results reported by Templeton and Weinberg[23,24] and by others in earlier studies. The first type of site is a very strong adsorption site that irreversibly adsorbs DMMP at these temperatures, associated with Lewis acid sites, while the second type of site is a more weakly adsorbing physisorption site, associated with Brønsted acid sites. Saturation of the chemisorption sites leads to the observation of the broad DMMP breakthrough curve, while saturation of both the chemisorption and physisorption sites leads to the strong, narrow peak.

From Figure 3B, it is clear that for DMMP doses of 70 μmol and greater, methanol evolution begins at the nearly the same time, regardless of dose. The results suggest that once the strongest adsorption sites are occupied by DMMP and DMMP breakthrough occurs, methanol produced by the decomposition reaction evolves from the bed with little interaction with the surface.

Figure 4 shows the amount of methanol observed as a function of the DMMP dose, where the total amount of methanol is taken to be the integrated methanol flow measured from the beginning of the experiment to slightly more than 20 h after the DMMP dose. The form of the data suggests that some threshold amount of DMMP is needed before methanol is observed. The data are fit to a function of the form

$$\mathrm{MeOH} = \frac{a(\mathrm{DMMP} - \mathrm{DMMP}_0)}{b + (\mathrm{DMMP} - \mathrm{DMMP}_0)} \qquad (1)$$

where MeOH is the amount, in μmol, of methanol observed after a dose, and DMMP is the number of μmol of DMMP dosed onto the surface, while DMMP_0 is the *x*-axis intercept in the figure, determined to be 24.3 μmol. Equation 1 is functionally equivalent to the Langmuir adsorption isotherm, indicating that the amount of methanol produced is proportional to the surface coverage of DMMP, after subtraction of the value DMMP_0. The limiting amount of methanol produced for exposure to an infinite amount of DMMP is represented by the constant *a* in eq 1 and is found to be 45.5 μmol. The constant *b* is related to the rate of rise of MeOH with DMMP dose amount. Experimentally, the amount of methanol observed after a flow of 467 μmol of DMMP was found to be 41.5 μmol, compared to a value of 42.5 μmol predicted by eq 1.

Variable Adsorbent/Fixed Dose. To lend further insight into the reactions occurring on the surface, a set of experiments was carried out in which variable amounts of adsorbent were dosed with a fixed amount of DMMP. The amounts of adsorbent tested were 15 mg, 30 mg, and 45 mg. The 15 and 45 mg samples were dosed with 20 μmol of DMMP, while two experiments were carried out with 30 mg of sample, one dosing it with 20 μmol and one with a 40 μmole dose.

For 15 mg of the adsorbent, 20 μmol of DMMP more than saturated the adsorbent, DMMP breakthrough was observed, and methanol was the only product observed; no dimethyl ether was found. For the same dose on 30 mg of adsorbent, no DMMP breakthrough was observed and both methanol and dimethyl ether were observed, although slightly less methanol was observed than for the 15 mg experiment. For 45 mg of adsorbent, for the same 20 μmole dose, only dimethyl was

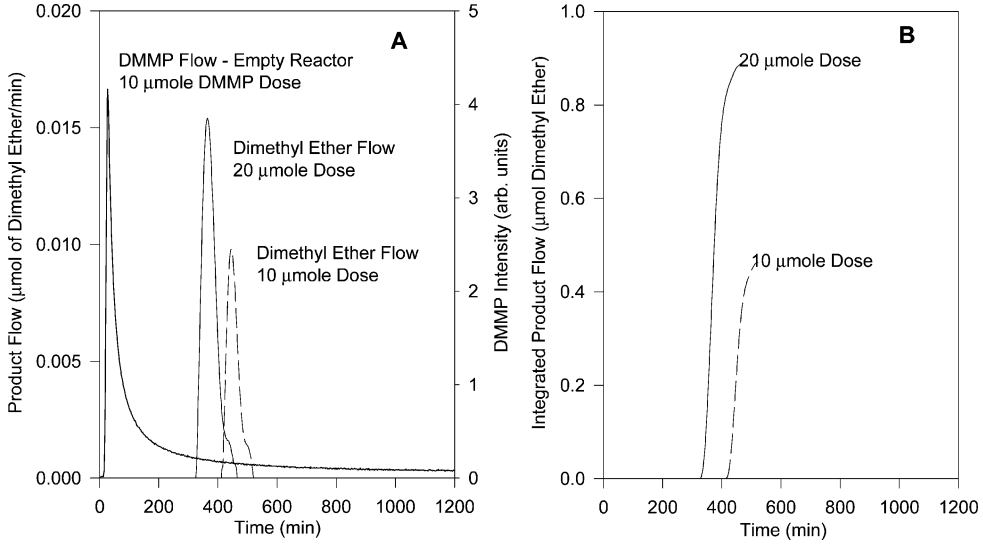

Figure 2. Product flow curves obtained by dosing the 20 wt % Ce on η-Al_2O_3 with (A) 10 and (B) 20 μmol of DMMP. Dimethyl ether is not observed until well after the bulk of the DMMP flow is over.

TABLE 1: Results from DMMP Dosing Experiments

DMMP exposure (μmol)	breakthrough time $(CH_3)_2O$ (min)	total $(CH_3)_2O$ production (μmol)	breakthrough time[a] MeOH (min)	total CH_3OH production (μmol)	breakthrough time DMMP (min)
10	421	0.5	NO	0.0	NO
20	331	0.9	NO	0.0	NO
30	183	3.1	346	7.6	NO
40	153	3.7	221	16.1	NO
50	161	3.7	231	18.0	NO
60	104	2.7	130	24.9	228
70	87	2.3	99	27.5	161
80	81	1.7	97	30.9	170
100	94	1.6	96	32.8	159
150	67	0.8	89	36.2	122
200	80	0.4	92	38.2	138

[a] NO: Not Observed

TABLE 2: Exposure of Different Amounts of Adsorbent to 20 μmol of DMMP

amount of adsorbent (mg)	production of dimethyl ether (μmol)	production of methanol (μmol)	breakthrough of DMMP
15	0	10.3	yes
30*	2.3/0.9	8.9/19.0	no/yes
45	2.2	0	no
60	0.9	0	no

[a] The value on the left is for exposure to 20 μmol of DMMP, the value on the right is for exposure to 40 μmol of DMMP.

observed as a product, and for 60 mg, as shown earlier, only dimethyl ether was observed. These results are summarized in Table 2. Notable among the results is the comparison of the amounts of dimethyl ether formed on dosing 30 mg of the adsorbent with 20 μmol or 40 μmol of DMMP. The amount of dimethyl ether observed dropped by more than a factor of 2 as the DMMP dose was increased from 20 to 40 μmol, while the observed methanol production increased by more than a factor of 2.

Incremental Dose/Single Adsorbent. A series of experiments was carried out in which a single adsorbent sample (60 mg) was exposed to successive doses of DMMP, 10 μmol at a time. Twenty-four h were allowed to elapse between each dose, with pure helium flowing between doses, and infrared spectra were collected continuously. The flow profiles of compounds from the reactor are shown in Figure 5.

From Figure 5A, after the first DMMP dose, dimethyl ether is relatively slow to evolve from the surface. Nearly 8 h elapse before dimethyl ether is observed. After subsequent doses, however, dimethyl ether is observed relatively quickly after the DMMP dose. As can be seen from Figures 5A and 6A, the amounts of dimethyl ether that evolve from the adsorbent bed after each DMMP dose are very similar to each other, ~0.5 μmol, until the eighth dose, after which no dimethyl ether was observed, nor was any observed for the two subsequent doses.

The observation of methanol on the other hand, Figure 5B, begins as a slow rise after the third dose, and after the fourth dose methanol appears in a series of spikes. This continues until the seventh dose, after which there is a peak at about 145 h followed by decreasing spikes of methanol observed after subsequent DMMP doses.

DMMP is not observed in the flow from the adsorbent bed until after the seventh dose, when it evolves slowly from the bed, Figure 5C. For subsequent doses, however, virtually all of the DMMP evolves from the adsorbent bed, having saturated the surface. The tabulated results, including the amounts of DMMP that evolve from the adsorbent bed, are shown in Table 3.

A comparison of the flow of dimethyl ether, Figure 5A, with that of DMMP, Figure 5C, shows that saturation of the surface by DMMP coincides with the end of the dimethyl ether production. It appears that dimethyl ether is formed at fresh surface sites found by each successive dose as the DMMP front

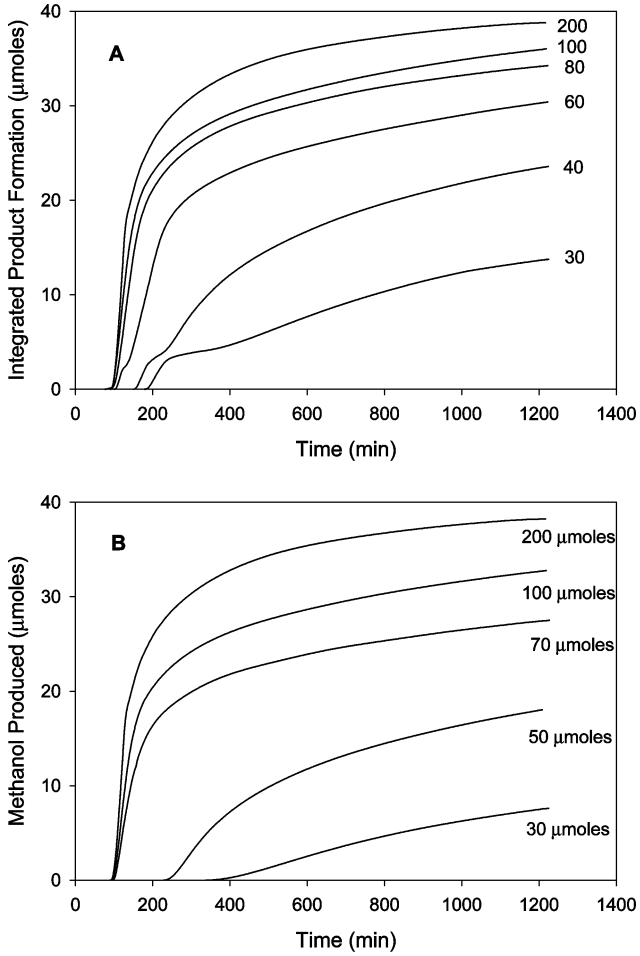

Figure 3. Product flow as a function of time for different dose amounts of DMMP on the 20 wt % Ce on η-Al_2O_3 adsorbent: (A) integrated total product flow (= 2*Me_2O + MeOH) and (B) integrated methanol flow.

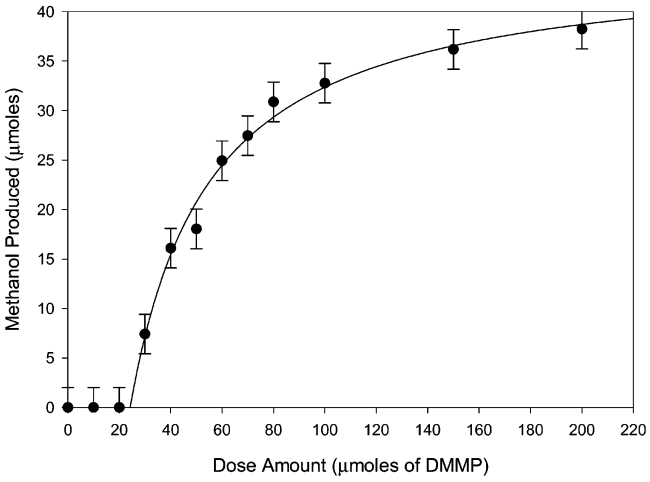

Figure 4. Amount of methanol produced as a function of DMMP dose. The experimental points are shown as the filled circles while a fit of the data to eq 1 is shown as a line.

moves through the adsorbent bed, and that once the free sites have been saturated, no more dimethyl ether is formed.

In Figure 5B it can be seen that methanol begins to evolve very slowly from the adsorbent bed after the third DMMP dose, but appears as a spike after the fourth dose. Each subsequent DMMP dose yields a spike of methanol that appears rapidly after the dose event. The slow evolution observed after the third

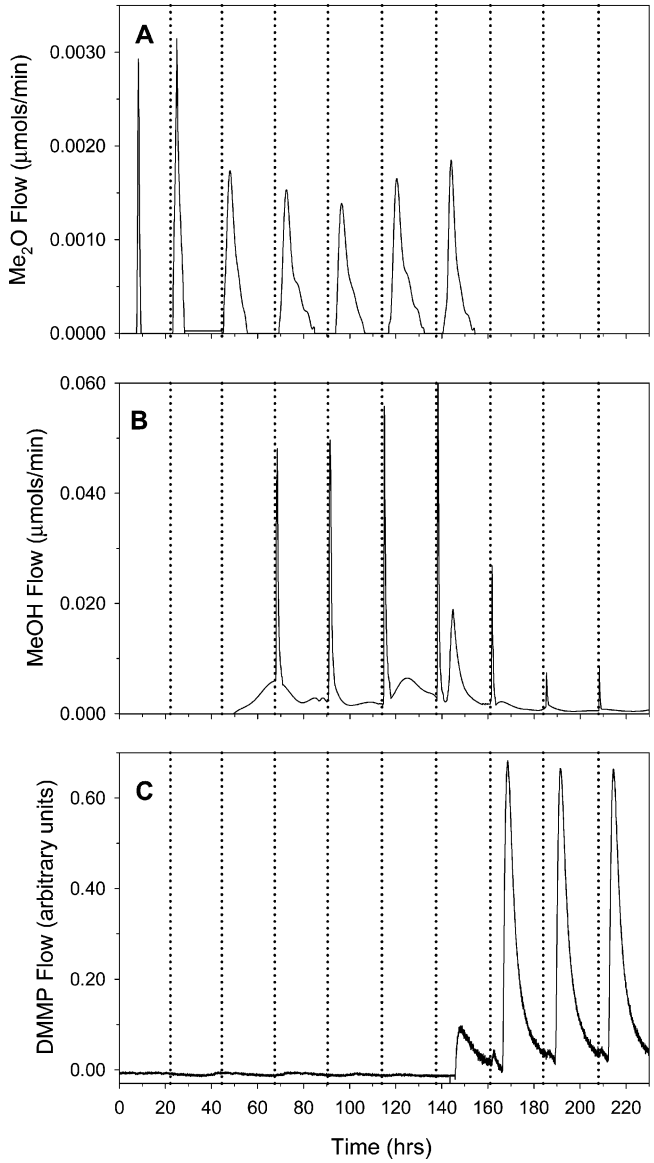

Figure 5. Flow of gas-phase compounds from the reactor during the incremental dose experiment. The dotted lines correspond to the times when DMMP doses were delivered to the sample.

dose is almost certainly due to the flow of methanol formed from the decomposition of the first doses of DMMP. This evolution is an indication that the strong methanol adsorption sites have been saturated with either adsorbed methanol or DMMP. Once these sites have been occupied, subsequent doses of DMMP lead to the observed spikes of methanol. There are undulations on the methanol background that correspond to methanol adsorbed at the strong adsorption sites slowly making its way out of the adsorbent bed. The peak that appears at approximately 145 h coincides with the breakthrough of DMMP, Figure 5C. Most of the methanol formed from the decomposition makes its way out of the adsorbent bed after the fourth, fifth, sixth, and seventh doses (Figure 6B).

DMMP Reaction with Adsorbed Methanol. When methanol is dosed by itself onto these CeO_x/Al_2O_3 adsorbents, a significant concentration of surface methoxy groups is formed, as shown by results from infrared diffuse reflectance spectroscopy studies, discussed later. An experiment was developed to examine the reaction of DMMP with a surface that had been saturated with methanol. Two different dosing experiments were performed. In the first, methanol was dosed onto an adsorbent sample (60

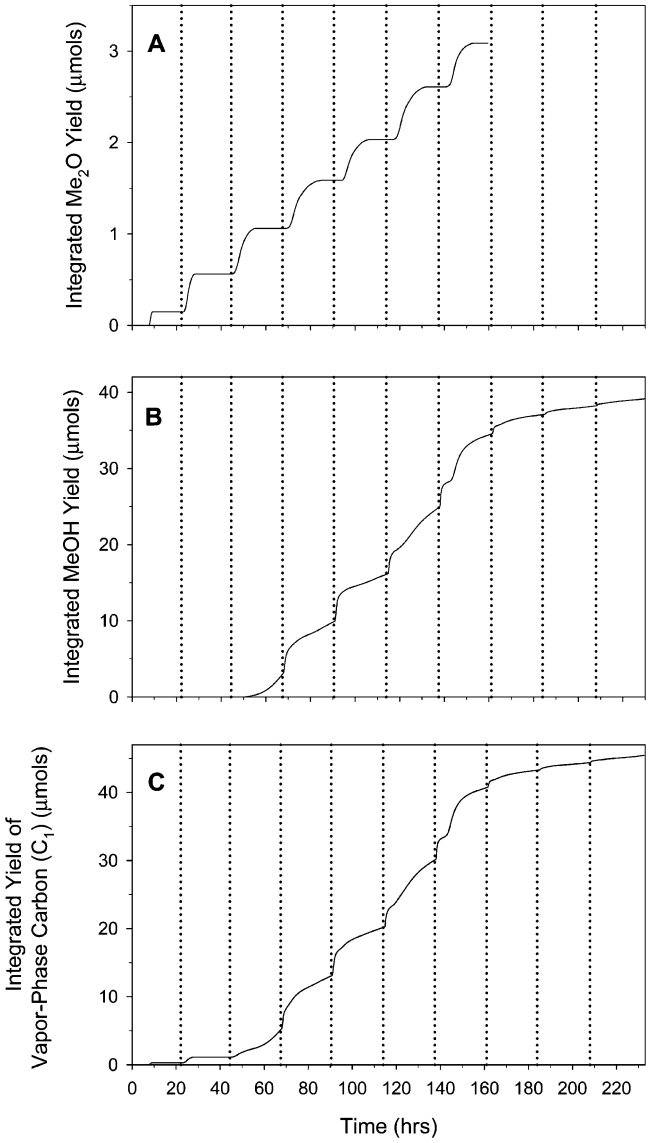

Figure 6. Integrated product yield from the incremental dose experiment. The dotted lines correspond to the times when DMMP doses were delivered to the sample.

TABLE 3: Amounts of Gas-Phase Products and DMMP Measured after Incremental Doses of DMMP[a]

dose (10 μmol increments)	dimethyl ether measured (μmol)	methanol measured (μmol)	DMMP measured (μmol)	total DMMP deficit (μmol)
1	0.2	0.0	0	9.6
2	0.4	0.0	0	18.8
3	0.5	3.2	0	24.6
4	0.5	7.2	0	26.4
5	0.5	6.8	0	28.6
6	0.6	8.8	0	28.6
7	0.5	10.0	2	25.6
8	0.0	2.2	9−9.5[b]	23.9
9	0.0	1.1	9−9.5	23.3
10	0.0	1.0	9−9.5	22.8

[a] Amounts shown are the integrated amounts measured beginning from the infrared spectrum collected just prior to dose *n* to the one collected just prior to dose *n*+1. [b] The higher value is used for DMMP deficit calculation.

mg) until methanol breakthrough was observed. After that time, the flow was switched to pure helium. The infrared spectra of the gas-phase effluent were obtained continuously for twenty-four h before and after saturation. In the second experiment, after saturation of the adsorbent by methanol, the sample was immediately dosed with 20 μmol of DMMP, followed by a flow of pure helium for twenty-four h. The methanol flow from the reactor measured for the two experiments was dramatically different.

The difference between the methanol flow observed after the addition of DMMP and that observed with no added DMMP is shown in Figure 7. The spike in the methanol flow occurs simultaneously with the addition of the DMMP pulse. The shoulder that appears prior to the spike is due a slightly earlier methanol breakthrough observed for the second experiment, due to small differences in sample packing and/or methanol flow. The total additional amount of methanol observed due to the added 20 μmol of DMMP was found to be in excess of 30 μmol, suggesting that a combination of surface reaction of DMMP to form methanol, perhaps involving surface methoxy groups, along with displacement of adsorbed methanol is needed to account for the observed results. No dimethyl ether was observed.

Methanol and Dimethyl Ether Reactions with Surface Fragments. To check for possible reactions between the reaction products dimethyl ether and methanol with surface fragments, a set of experiments was carried out in which a small fixed amount of DMMP was allowed to flow onto the adsorbent, followed by methanol or dimethyl ether. In these experiments, 20 μmol of DMMP was first dosed onto 60 mg of the adsorbent, 24 h were allowed to elapse to recover reaction products, then 20 μmol of dimethyl ether or methanol was dosed onto the adsorbent. Twenty μmol is not enough to saturate 60 mg of the adsorbent with DMMP, and, consistent with the other results, only dimethyl ether was observed after the DMMP dose, in the amount of 0.5−1.0 μmol. In the reaction involving added dimethyl ether, no methanol was observed after the addition of dimethyl ether. For the reaction involving added methanol, a small additional amount of dimethyl ether was observed after the addition of methanol. The additional amount was in the form of a pulse of dimethyl ether which, when integrated, was found to correspond to approximately 0.1 μmol.

Infrared Diffuse Reflectance Studies. The infrared spectra that result from DMMP adsorbing on the alumina-supported cerium oxide are shown in Figure 8. Included for comparison is the spectrum for adsorbed methanol. Figure 8A shows the C−H stretching region of the infrared spectrum, while Figure 8B shows the lower frequency region between 1500 and 1000 cm^{-1} (infrared absorption by the alumina substrate prevents examination of frequencies below 1000 cm^{-1}). Three bands are found in the C−H region of the spectrum at 2808, 2888, and 2916 cm^{-1}, and a shoulder at 2945 cm^{-1}. The infrared spectrum for adsorbed methanol on the alumina-supported cerium oxide is included in the figure and is very similar to that obtained by Badri et al. for methanol on polycrystalline ceria.[39] Lamotte et al. had previously shown that methanol adsorbs dissociatively at room temperature on polycrystalline cerium oxide with cleavage of the O−H bond,[40] and as a result Badri et al. assigned the bands observed in their study to methoxy groups adsorbed in either an on-top (monocoordinate) configuration or as doubly or triply bridging species. Bands that were associated with intact methanol molecules were observed only for large doses of methanol onto the polycrystalline ceria. Samples pretreated at 400 °C yielded primarily on-top or doubly bridging species, with approximately 1:1 to 2:1 relative amounts of the on-top to bidentate species, and with the tridentate species accounting for only 10% or less of the total amount of the surface methoxy species.

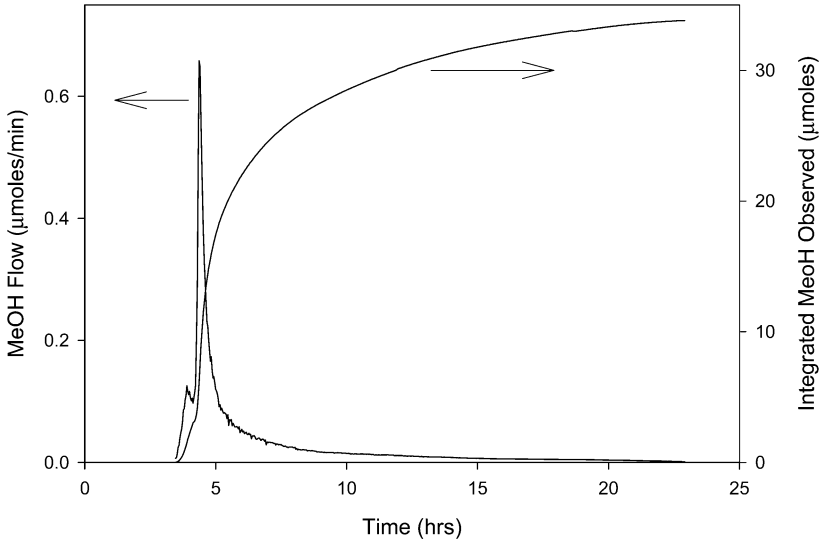

Figure 7. Increase in methanol flow observed due to a 20 μmole dose of DMMP after saturating an adsorbent with methanol. The curves are determined from the subtraction of two experiments, the first involving saturating an adsorbent sample with methanol followed by a flow of pure helium. The second experiment saturated an adsorbent sample with methanol, then followed with a dose of 20 μmol of DMMP, and again with a flow of pure helium.

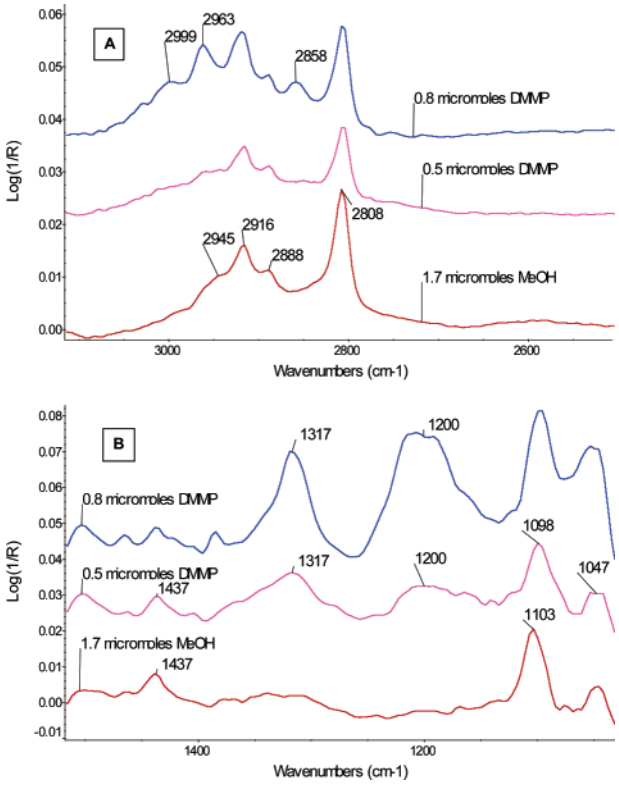

Figure 8. Infrared diffuse reflectance spectra of methanol and DMMP adsorbed on the alumina-supported cerium oxide adsorbent. Figure 8A shows the region that includes the C−H stretching vibrations of the methyl and methoxy groups. Figure 8B shows the region that includes the C−O stretch, the P−CH_3 deformation, and the P−O stretch vibrations. The curves are referenced to the same vertical scale, but have been offset to aid viewing.

The frequencies noted for the different vibrational modes of the adsorbed methoxy group are shown in Table 4. Included in the table are the results from Badri et al., as well as the methoxy-group frequencies observed for the alumina-supported cerium oxide: absorption frequencies observed after methanol adsorption, and those that result from the initial adsorption of DMMP. The frequency differences between absorption bands due to the monocoordinate (I) and doubly bridging (II) species are small,

TABLE 4: Infrared Absorption Frequencies (cm^{-1}) for Methoxy Group on Cerium Oxide

	surface methoxy (Badri et al.)	surface methoxy (this work)	adsorbed DMMP
$\nu_a(CH_3)$	2911	2916	2916
$2\delta(CH_3)$	2883	2888	2889
$\nu_s(CH_3)$	2803	2808	2806
$\delta(CH_3)$	1434	1437	1437
ν(OC) (I)	1108	1103	1098
ν(OC) (II)	1065	1048	1047

less than the spectral resolution of our experiments, except for the O−C stretching (ν(OC)) mode, and this is the only mode for which differences between these two species are noted in Table 4. As can be seen, the similarities between the absorption frequencies observed for the methoxy group formed when methanol is dosed onto the adsorbent surface, and the absorptions observed when DMMP is first dosed onto the surface leave little doubt that the methoxy group is formed upon adsorption of DMMP. The one significant difference in the work of Badri et al. and the current work has to do with the frequency of the O−C stretching vibration of the bridging species. The lower frequency observed for the bridging methoxy species in the current work may be due to the fact that some of the bridging species are bridging between cerium and aluminum species on the adsorbent surface.

As DMMP continues to be added to the adsorbent, the bands due to molecular DMMP can be observed at 2999, 2963, and 2858 cm^{-1}.[4] The methoxy group band at 2916 cm^{-1} overlaps and obscures the molecular DMMP absorption at 2926 cm^{-1}.

The lower frequency region includes a strong absorption band due to the deformation vibration of the methyl group bound directly to the phosphorus atom of DMMP, observed at 1317 cm^{-1}. As can be seen, it appears that this band is present after the initial doses of DMMP, even though there is no clear evidence for the corresponding C−H stretching vibrations of this group (at 2999 and 2926 cm^{-1}). The C−H stretch absorptions of this group are relatively broad, however, and may be obscured at these low concentrations under the methoxy group absorptions. A broad band at approximately 1200 cm^{-1} is also observed, and this band is due to the adsorbed phosphorus−oxygen stretching vibration of the phosphorus-containing DMMP fragment.

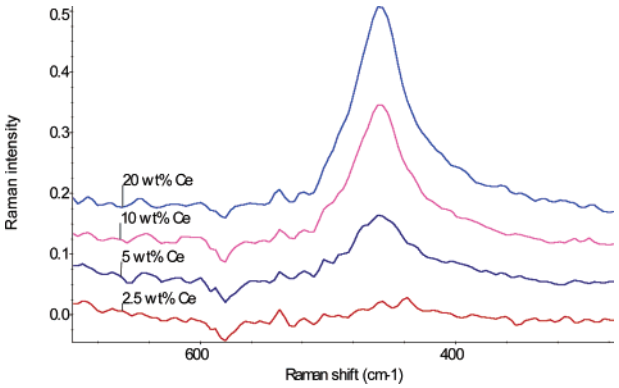

Figure 9. FT-Raman spectra in the region of the CeO_2 F_{2g} mode of the alumina-supported cerium oxide adsorbents as a function of cerium loading. The curves are referenced to the same vertical scale, but have been offset to aid viewing.

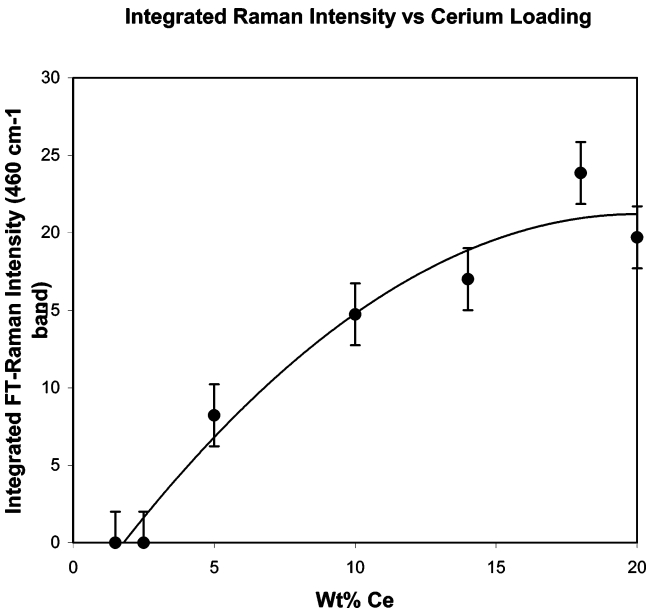

Figure 10. Integrated intensity of the CeO_2 FT-Raman band as a function of cerium loading. The curve shown on the plot is included as a guide to the approximate behavior of the intensity as a function of Ce loading on the samples and is not based on any model of Raman intensity as a function of CeO_2 concentration for these samples.

The infrared diffuse reflectance results show that when DMMP adsorbs on the alumina-supported cerium oxide surfaces at room temperature, the dominant process for the initial species adsorbed is decomposition to yield a surface methoxy group and a phosphorus-containing fragment. In their work on titania surfaces,[41,42] Rusu and Yates observed the formation of surface methoxy groups from adsorbed DMMP on titania at temperatures in excess of 214 K. In the current study, the infrared spectra provide information not only indicating the formation of the methoxy group but also suggesting its location.

The infrared spectra that result from methanol interacting with a variety of metal oxide surfaces, both bulk oxides and supported oxides, have been recently reviewed by Burcham et al.[43,44] In that work, the adsorption of methanol on alumina is shown to yield two sets of bands, one set belonging to a surface methoxy group (2941 and 2820 cm^{-1}) and a second set assigned to a Lewis-bound intact methanol molecule (2955 and 2839 cm^{-1}). Neither of these sets of bands agrees with the bands observed in the current work (2916 and 2808 cm^{-1}) but, as shown in Table 4, the current results agree very well with the bands observed for methoxy groups on polycrystalline ceria. The results leave little doubt that when DMMP adsorbs on the alumina-supported cerium oxide, the methoxy groups that are formed are associated predominantly with the cerium oxide phase. As suggested above, the lower frequency for the C−O stretch vibration for the bridging species may be the result of the formation of a methoxy group that bridges between the ceria and alumina phases.

FT-Raman Studies. As discussed in an earlier publication, FT-Raman spectroscopy can provide significant information regarding the nature of a supported cerium oxide phase.[27] The presence of a band at approximately 464 cm^{-1} corresponding to the F_{2g} mode of crystalline CeO_2 indicates the formation of a three-dimensional CeO_2 phase.[45−47] The intensity of the Raman band is proportional to the amount of crystalline CeO_2 on the support surface. The width of this band can be related to the size of the crystal domains.[46−49] In addition, the frequency of the band maximum is also sensitive to the size of the crystallites. As a way of examining the nature of the alumina-supported cerium oxide, the FT-Raman spectra of a series of alumina-supported cerium oxide samples, using η-alumina as the substrate, were measured, using cerium loadings of from 1.5 wt % Ce to 20 wt % Ce. The goal was to examine the onset of crystallite formation as a function of cerium loading for these adsorbents, and compare that to the measured DMMP decomposition yields for the same materials, similar to the analysis that was carried out in the earlier study.[27] FT-Raman spectra observed for representative adsorbents are shown in Figure 9. The band shown corresponds to the F_{2g} mode of crystalline CeO_2 discussed above. In the spectra shown, the peak maxima all occur near 459 cm^{-1} and the full width at half-maximum (fwhm) values are found to be approximately 44 cm^{-1}. The fwhm may be slightly larger for the 5 wt % Ce sample than for the higher weight loading samples, but not more than 10% higher. The integrated intensity of the band for the entire series as a function of cerium loading is shown in Figure 10. As can be seen, the lowest weight loadings show no contribution from this band, but for cerium loadings of 5 wt % and greater, an increase in the integrated intensity as a function of cerium loading is observed.

For the 5 wt % Ce through 20 wt % Ce alumina-supported cerium oxide samples examined, the 459 cm^{-1} FT-Raman band was found to have a fwhm value of approximately 44 cm^{-1}. As shown in the work by Zhang et al.,[48] for small cerium oxide crystals the width of the Raman band is a sensitive function of the particle size. The similarity of the fwhm values found in the current work suggests that the materials contain similarly sized cerium oxide crystallites, with a greater or smaller number of them depending on the amount of cerium used in the formulation. A comparison of the fwhm values and the peak positions found here to those found by Zhang et al. suggests that the alumina-supported cerium oxide particles have a crystal size of less than six nanometers (<6 nm). Additionally, the FT-Raman bands observed in the current study show the low-frequency asymmetry seen by Zhang and co-workers for nanoparticulate cerium oxide. For the 2.5 wt % cerium on alumina adsorbent, however, the absence of a Raman band cannot rule out the presence of crystallites with a size of 1 nm or less.[45]

Decomposition Yield vs Cerium Loading. Figure 11 shows the integrated amount of methanol formed after exposure to a total flow of 760 μmol of DMMP for the same set of adsorbents as examined in Figure 10. A dramatic increase in methanol formation with cerium content is observed for the lowest loadings, followed by a slower increase in product formation with cerium content after a loading of approximately 5 wt %

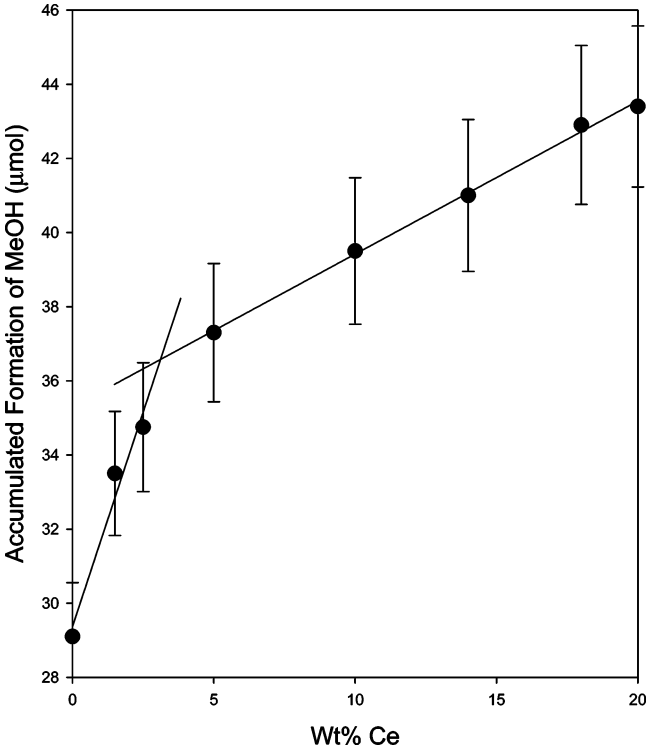

Figure 11. Total methanol yield after exposure to 760 μmol of DMMP for several different alumina-supported cerium oxide adsorbents as a function of cerium loading.

Ce. These results taken together, the FT-Raman intensity vs cerium content and the decomposition yield vs cerium content, are similar to those observed in our earlier study of cerium and iron coimpregnated oxides on γ-alumina and indicate that the most active form of the supported cerium oxide is the dispersed form, with the cerium oxide in the form of CeO_2 crystallites yielding a slower increase in the decomposition yield.[27]

Discussion

One aspect of the observed behavior in the microreactor experiments can be explained by the relative affinities of the three different gas-phase species, dimethyl ether, methanol, and DMMP, for the adsorbent surface. There are surface sites that adsorb dimethyl ether relatively strongly, but their number is limited. Methanol interacts much more strongly with the surface, moving more slowly through the adsorbent bed and taking much longer to evolve from the bed. DMMP, however, interacts so strongly with the adsorbent that it replaces dimethyl ether and even the strongly adsorbed methanol at surface sites.

In the variable dose/fixed adsorbent experiment (Figures 1, 3, and 4), the dramatic absence of methanol from the decomposition of DMMP for the smaller doses is due to the methanol being strongly adsorbed at empty surface sites on these samples. This is the simplest explanation for the low methanol yield in these experiments, and it is the only one that makes sense for the second set of experiments, the fixed dose/variable adsorbent experiments (see Table 2). In those experiments, a 20 μmol DMMP dose onto 15 mg of adsorbent generates more than 10 μmol of methanol, while the same DMMP dose onto 45 mg of adsorbent generates no methanol. With the larger adsorbent samples, 45 and 60 mg, the amount of methanol formed from a 20 μmol dose of DMMP is not enough to saturate the strong methanol adsorption sites, and as a result no methanol is observed. For the experiments with smaller amounts of adsorbent, 15 and 30 mg of adsorbent, the combination of DMMP and methanol saturates the strong methanol adsorption sites and methanol is observed. For 15 mg of the adsorbent, 20 μmol of DMMP saturates the adsorbent bed, and all the methanol formed is recovered, while for the experiment using 30 mg of the adsorbent and the same amount of DMMP, DMMP breakthrough is not observed, so some of the methanol produced is adsorbed at strong adsorption sites.

SCHEME 2

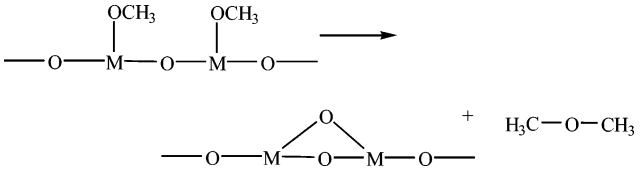

Proposed Mechanism for Product Formation. The results that point to a distinct mechanism for product formation from the DMMP decomposition have to do with the formation of dimethyl ether. The results shown in Figure 1, as well as the results for 30 mg of adsorbent shown in Table 2, show that the production of dimethyl ether is significantly reduced for DMMP doses that more than saturate the adsorbent bed, and the larger the dose, the lower the amount of dimethyl ether observed, even as the amount of methanol observed increases. These results suggest that the reaction path that forms dimethyl ether and the one that forms methanol compete with one another.

When DMMP adsorbs on these adsorbent surfaces, a significant fraction of the DMMP decomposes to form adsorbed methoxy groups and phosphorus-containing fragments. This decomposition has been found to occur as DMMP adsorbs on other surfaces,[23,27,29] and is clearly indicated for the CeO_x/Al_2O_3 adsorbent by the results from the infrared diffuse reflectance spectroscopy studies. It is suggested that competition for these surface methoxy groups gives rise to the observed changes in product distribution.

There are several possible scenarios involving a surface methoxy intermediate that lead to the formation of dimethyl ether, but it is suggested that the most likely one is that dimethyl ether is formed from the combination of two neighboring methoxy fragments (Scheme 2). Modification of the surface chemistry by the presence of DMMP or DMMP fragments appears to be important with regard to this reaction. As noted earlier, methanol dosed by itself onto the adsorbent surface does not form measurable amounts of dimethyl ether, even though it does form significant numbers of surface methoxy groups, as seen in infrared diffuse reflectance spectroscopy experiments.

Two other plausible paths for dimethyl ether formation are the reaction of the surface methoxy groups with either methanol produced from the decomposition of DMMP or with DMMP itself. As presented in the results section, methanol can react with surface DMMP or fragments to yield dimethyl ether, but this is probably not the primary path. If it were, it would suggest that as the methanol concentration increases, the dimethyl ether yield should increase as well, the opposite of what is observed. At a minimum, the observed dimethyl ether yield should not decrease as the DMMP dose increases, which is what is observed in Figure 1B. Also, in Figure 5, A and B, the dimethyl ether flow for doses 4−7 appears *after* the spikes in the methanol flow, suggesting that the formation of dimethyl ether is independent of the methanol flow. With regard to the reaction of DMMP with surface fragments, no dimethyl ether was formed when DMMP was dosed onto a surface saturated with methanol.

For DMMP doses that exceed the amount needed to saturate the surface, all of the surface methoxy groups are exposed to vapor-phase DMMP, and the larger the dose, the higher the

SCHEME 3

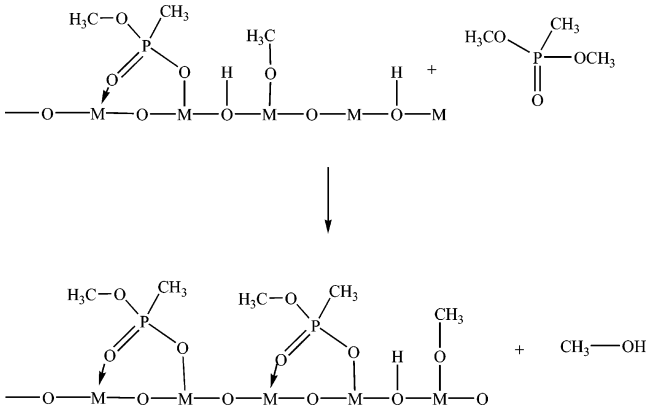

DMMP concentration that these groups see. The proposed interaction of surface methoxy groups with DMMP to form methanol would account for the drop in dimethyl ether formation observed for large doses and the simultaneous increase in methanol (Scheme 3). In Scheme 3 is shown what we believe to be the most likely path for the formation of methanol on these surfaces, with as much detail as the results allow. In this scheme, the interaction between adsorbing DMMP molecules and surface methoxy groups leads to the formation of vapor-phase methanol. The DMMP molecule, acting as a strong Lewis base, provides the driving force for the reaction between the surface methoxy group and a surface hydroxyl group. It seems unlikely, although it is possible, that the hydrogen needed to form methanol comes from the DMMP molecule.

Scheme 3 can be used to explain the results from the variable adsorbent/fixed dose experiments as follows. In the experiment dosing 15 mg of the adsorbent with 20 μmol of DMMP, a relatively small amount of time elapses between the initial formation of the surface methoxy groups and the saturation of the available surface with DMMP. Thus, the surface methoxy groups that are formed are exposed to relatively high concentrations of vapor-phase DMMP, giving rise to methanol, before significant amounts of dimethyl ether can be formed. On the other hand, in the experiments with 20 μmol of DMMP adsorbing on 30 and 45 mg of adsorbent, there are methoxy groups that are not exposed to vapor phase DMMP at all, and dimethyl ether has time to form. The methanol that is formed during the 45 mg adsorbent experiment is either irreversibly adsorbed or so strongly bound to the adsorbent that it evolves only very slowly from the adsorbent bed.

These models for the reaction also explain the results observed for the incremental dose experiment (Figure 5). When the first dose of DMMP is added, surface methoxy groups are formed which subsequently react with each other to form dimethyl ether, or with DMMP to form methanol. The methanol is strongly adsorbed and progresses only slowly through the bed, while the dimethyl ether is held more weakly and eventually makes its way through the bed. A narrow band at the front of the bed is saturated with DMMP by the first dose, while a greater fraction of the bed has been saturated with methanol, since it is less strongly held, and the entire bed has been saturated with dimethyl ether, since it has made its way out of the adsorbent bed. Each new addition of DMMP moves the DMMP front further through the adsorbent bed and produces primarily methanol along with a small amount of dimethyl ether, until the surface has been saturated with DMMP or DMMP fragments. After the third dose, methanol appears in the infrared cell, indicating that the strong methanol sites have been saturated. The methanol spikes that are seen for the fourth and subsequent doses are probably due to two different but virtually indistinguishable processes: methanol being replaced at the strong adsorption sites by added DMMP, and the production of new methanol by the reaction of added vapor-phase DMMP with surface methoxy groups.

After saturation of the surface by DMMP, no more dimethyl ether is formed. Methanol, however, continues to be observed through the reaction of remaining surface methoxy groups with added DMMP, or replacement of surface-adsorbed methanol with DMMP.

Comparing results from the incremental dose experiment with the single dose experiment provides an interesting test of the model. For DMMP dose amounts that saturate or more than saturate the adsorbent, the incremental dose experiment should form more dimethyl ether than does the single dose experiment, with the larger single doses yielding the smallest amounts of dimethyl ether. Thus, for 60 mg of adsorbent exposed to 70 μmol of DMMP, the incremental dose experiment forms 3.1 μmol of dimethyl ether, while the single dose experiment forms 2.3 μmol, a single 100 μmol dose forms 1.6 μmol, and a single 200 μmol dose forms only 0.4 μmol of dimethyl ether.

The fit of the data to a modified Langmuir adsorption isotherm, eq 1, is consistent with the idea that the reaction is stoichiometric, not catalytic, and the formation of methanol is limited by the availability of surface sites. The interpretation of the intercept $DMMP_o$ found in Figure 4, 24.3 μmol, is that approximately 24 μmol of DMMP dosed onto the surface, with the corresponding amount of methanol formed by DMMP decomposition, saturates the strong methanol adsorption sites.

As mentioned in the Introduction, one of the goals of these experiments was to develop a method for assessing the amount of DMMP either decomposed or irreversibly adsorbed on these adsorbents through the measurement of gas-phase products. From the data contained in Table 3 and the assumed reaction stoichiometry, it is possible to calculate the amount of DMMP unaccounted for after each dose. The calculated deficit amount is shown in Table 3. The average DMMP deficit, after the third dose, is approximately 25 μmol, suggesting that 25 μmol of DMMP is strongly adsorbed at these temperatures but does not give rise to gas-phase products. A similar calculation could be carried out using data from Table 1 if accurate DMMP breakthrough amounts were available. However, the DMMP breakthrough amount for the largest doses is 50−150 μmol, and we do not have confidence in the accuracy of the DMMP breakthrough measurements calculated for the large doses. From these data, it can be determined that the decomposition capacity of 60 mg of the adsorbent is approximately 46.4 μmol of DMMP, leading to the formation of 40.2 μmol of methanol and 3.1 μmol of dimethyl ether, although the product branching ratio will depend on the dosing protocol. An additional amount of approximately 25 μmol of DMMP is apparently very strongly adsorbed, although some of this amount may very slowly evolve from the adsorbent.

Conclusion

Methanol and dimethyl ether formed by the decomposition of DMMP as it adsorbs on an alumina-supported cerium oxide adsorbent at 25 °C appear to form through competitive processes involving surface-bound methoxy groups. It is proposed that dimethyl ether is formed by the reaction between two surface methoxy groups, while the reaction that yields methanol is driven by the interaction between DMMP and surface methoxy groups. The observed results do not completely eliminate the participation of other routes in the formation of methanol.

The surface methoxy groups that are formed when DMMP adsorbs on the alumina-supported cerium oxide adsorbent are attached to cerium oxide domains. The cerium domains that are the most active for DMMP decomposition appear to be either two-dimensional domains or small (<1 nm) crystallites, with somewhat larger (<6 nm) crystallites contributing to DMMP decomposition but not as strongly on a per cerium basis. The onset of crystallite formation appears to coincide to a surface concentration of approximately 0.6 Ce atoms per nm^2, a concentration that, as discussed in an earlier publication, is relatively low compared to the onset for crystallite formation for other alumina-supported metal oxides.[27]

The new cerium oxide on alumina adsorbent that has been developed decomposes approximately 775 μmol of DMMP per gram of adsorbent at 25 °C, making it the most active reactive adsorbent material for ambient temperature applications that have been reported in the literature. It also has an apparent capacity for strong DMMP adsorption of approximately 400 μmol, yielding an apparent total capacity for DMMP of 1.1−1.2 mmol per gram of adsorbent.

Acknowledgment. The authors thank Dr. Mark G. White of the Georgia Institute of Technology for helpful discussions. The authors gratefully acknowledge support of the U. S. Army, Edgewood Chemical Biological Center, for support of this research. Also, the authors acknowledge the support of NASA through the High Performance Polymers and Composites Center.

References and Notes

(1) Ekerdt, J. G.; Klabunde, K. J.; Shapley, J. R.; White, J. M.; Yates, J. T., Jr. *J. Phys. Chem.* **1988**, *92*, 6182.
(2) Bowen, J. M.; Powers, C. R.; Ratcliffe, A. E.; Rockley, M. G.; Hounslow, A. W. *Environ. Sci. Technol.* **1988**, *22*, 1178.
(3) Cao, L.; Segal, S. R.; Suib, S. L.; Tang, X.; Satyapal, S. *J. Catal.* **2000**, *194*, 61.
(4) Mitchell, M. B.; Sheinker, V. N.; Mintz, E. A. *J. Phys. Chem. B* **1997**, *101*, 11192.
(5) Graven, W. M.; Weller, S. W.; Peters, D. L. *I. E. C. Process Des. Dev.* **1966**, *5*, 183.
(6) Tzou, T. Z.; Weller, S. W. *J. Catal.* **1993**, *146*, 370.
(7) Lee, K. Y.; Houalla, M.; Hercules, D. M.; Hall, W. K. *J. Catal.* **1994**, *145*, 223.
(8) Li, Y. X.; Koper, O.; Atteya, M.; Klabunde, K. J. *Chem. Mater.* **1992**, *4*, 323.
(9) Li, Y. X.; Schlup, J. R.; Klabunde, K. J. *Langmuir* **1991**, *7*, 1394.
(10) Li, Y. X.; Klabunde, K. J. *Langmuir* **1991**, *7*, 1388.
(11) Jiang, Y.; Decker, S.; Mohs, C.; Klabunde, K. J. *J. Catal.* **1998**, *180*, 24.
(12) Smentkowski, V. S.; Hagans, P.; Yates, J. T., Jr. *J. Phys. Chem.* **1988**, *92*, 6351.
(13) Guo, X.; Yoshinobu, J.; Yates, J. T., Jr. *J. Phys. Chem.* **1990**, *94*, 6839.
(14) Obee, T. N.; Satyapal, S. *J. Photochem. Photobiol. A: Chem.* **1998**, *118*, 45.
(15) Rusu, C. N.; Yates, J. T., Jr. *J. Phys. Chem. B* **2000**, *104*, 12299.
(16) Segal, S. R.; Suib, S. L.; Tang, X.; Satyapal, S. *Chem. Mater.* **1999**, *11*, 1687.
(17) O'Shea, K. E. *J. Photochem. Photobiol. A* **1997**, *107*, 325.
(18) Kanan, S. M.; Tripp, C. P. *Langmuir* **2001**, *17*, 2213.
(19) Bertilsson, L.; Potje-Kamloth, K.; Liess, H.-D.; Engquist, I.; Liedberg, B. *J. Phys. Chem. B* **1998**, *102*, 1260.
(20) Bertilsson, L.; Engquist, I.; Liedberg, B. *J. Phys. Chem. B* **1997**, *101*, 6021.
(21) Bertilsson, L.; Potje-Kamloth, K.; Liess, H.-D. *Thin Solid Films* **1996**, *284*−*285*, 882.
(22) Oh, S. W.; Kim, Y. H.; Yoo, D. J.; Oh, S. M.; Park, S. J. *Sens. Actuators B*, **1993**, *13*−*14*, 400.
(23) Templeton, M. K.; Weinberg, W. H. *J. Am. Chem. Soc.* **1985**, *107*, 97.
(24) Templeton, M. K.; Weinberg, W. H. *J. Am. Chem. Soc.* **1985**, *107*, 774.
(25) Tesfai, T. M.; Sheinker, V. N.; Mitchell, M. B. *J. Phys. Chem. B* **1998**, *102*, 7299−7203.
(26) Sheinker, V. N.; Mitchell, M. B. *Chem. Mater.* **2002**, *14*, 1257−1268.
(27) Mitchell, M. B.; Sheinker, V. N.; Tesfamichael, A. B.; Gatimu, E. N.; Nunley, M. *J. Phys. Chem. B* **2003**, *107*, 580−586.
(28) Aurian-Blajeni, B.; Boucher, M. M. *Langmuir* **1989**, *5*, 170.
(29) Rusu, C. N.; Yates, J. T., Jr. *J. Phys. Chem. B* **2000**, *104*, 12292.
(30) Henderson, M. A.; Jin, T.; White, J. M. *J. Phys. Chem.* **1986**, *90*, 4607.
(31) Hegde, R. I.; Greenlief, C. M.; White, J. M. *J. Phys. Chem.* **1985**, *89*, 2886.
(32) Wagner, G. W.; Procell, L. R.; O'Connor, R. J.; Munavalli, S.; Carnes, C. L.; Kapoor, P. N.; Klabunde, K. J. *J. Am. Chem. Soc.* **2001**, *123*, 1636.
(33) Wagner, G. W.; Bartram, P. W.; Koper, O.; Klabunde, K. J. *J. Phys. Chem. B*, **1999**, *103*, 3225.
(34) Wagner, G. W.; Koper,.; Lucas, E.; Decker, S.; Klabunde, K. J. *J. Phys. Chem. B* **2000**, *104*, 5118.
(35) Zhanpeisov, N. U.; Zhidomirov, G. M.; Yudanov, I. V.; Klabunde, K. J. *J. Phys. Chem.* **1994**, *98*, 10032.
(36) Soria, J.; Coronado, J. M.; Conesa, J. C. *J. Chem. Soc., Faraday Trans.* **1996**, *92*, 1619.
(37) Fernandez-Garcia, M.; Gomez Rebollo, E.; Guerrero Ruiz, A.; Conesa, J. C.; Soria, J. *J. Catal.* **1997**, *172*, 146−159.
(38) Tesfai, T. M.; Sheinker, V. N.; Mitchell, M. B. *J. Phys. Chem. B* **1998**, *102*, 7299−7203.
(39) Badri, A.; Binet, C.; Lavalley, J. C. *J. Chem. Soc., Faraday Trans.* **1997**, *93*, 1159−1168.
(40) Lamotte, J.; Moravek, V.; Bensitel, M.; Lavalley, J. C. *React. Kinet. Catal. Lett.* **1988**, *36*, 113.
(41) Rusu, C. N.; Yates, J. T., Jr. *J. Phys. Chem. B* **2000**, *104*, 12292−12298.
(42) Rusu, C. N.; Yates, J. T., Jr. *J. Phys. Chem. B* **2000**, *104*, 12299−12305.
(43) Burcham, L. J.; Briand, L. E.; Wachs, I. E. *Langmuir* **2001**, *17*, 6175−6184.
(44) Burcham, L. J.; Briand, L. E.; Wachs, I. E. *Langmuir* **2001**, *17*, 6164−6174.
(45) Martínez-Arias, A.; Fernández-Garcia, M.; Salamanca, L. N.; Valenzuela, R. X.; Conesa, *J. Phys. Chem. B* **2000**, *104*, 4038−4046.
(46) Shyu, J. Z.; Weber, W. H.; Gandhi, H. S. *J. Phys. Chem.* **1988**, *92*, 4964−4970.
(47) Larrson, P.-O.; Andersson, A. *J. Catal.* **1998**, *179*, 72−89.
(48) Zhang, F.; Chan, S.-W.; Spanier, J. E.; Apak, E.; Jin, Q.; Robinson, R. D.; Herman, I. P. *Appl. Phys. Lett.* **2002**, *80*, 127−129.
(49) Spanier, J. E.; Robinson, R. D.; Zhang, F.; Chan, S.-W.; Herman, I. P. *Phys. Rev. B* **2001**, *64*, 245407.